

# A Hybrid Open-Framework Structure Containing Different Manganese Phosphate Chains as Its Building Blocks

Lindong Luan,<sup>†</sup> Hejun Ding,<sup>‡</sup> Meng Yang,<sup>‡</sup> Zhien Lin,<sup>\*,‡</sup> and Hui Huang<sup>\*,†</sup>

<sup>†</sup>School of Chemistry, Beijing Institute of Technology, Beijing 100081, People's Republic of China

<sup>‡</sup>College of Chemistry, Sichuan University, Chengdu 610064, People's Republic of China

## S Supporting Information

**ABSTRACT:** An open-framework hybrid solid with two different types of manganese phosphate chains has been synthesized under solvent-free conditions. A type I chain consists of isolated  $\text{Mn}_2\text{O}_{10}$  dimers, while a type II chain contains an infinite  $\text{Mn}-\text{O}-\text{Mn}$  chain constructed from corner-sharing  $\text{Mn}_2\text{O}_{10}$  dimers. The compound shows ferrimagnetic behavior, which is different from the antiferromagnetic behavior for its structural analogue that only contains type I manganese phosphate chains.

Crystalline open-framework hybrid solids have been extensively studied because of their potential applications in catalysis, gas storage, separation, cathode materials, and sensing.<sup>1</sup> They emerge as an important class of solid-state materials by integrating both the compositional and structural features of zeotype inorganic solids and metal–organic frameworks.<sup>2</sup> During the past years, great efforts have been made to synthesize new metal phosphate–carboxylates under hydrothermal conditions.<sup>3</sup> These hybrid compounds display some interesting structural features and appealing physical properties such as magnetism and luminescence. An illustrative example is the gallium phosphate–oxalate NTHU-6 emitting yellow luminescence with high photoluminescence quantum efficiency.<sup>3c</sup>

The development of new strategies for the synthesis of crystalline materials is of great importance.<sup>4</sup> Compared with the hydrothermal method, solvent-free synthesis exhibits several advantages, such as reduced pollution, decreased system pressure, low cost, simple processing, and ease of handling.<sup>5</sup> Because the competition between solvent–framework and template–framework interactions is eliminated under solvent-free conditions, the crystallization pathway for open-framework structures may be different from that of hydrothermal synthesis. In particular, some new secondary building blocks may be produced under solvent-free conditions. Thus, solvent-free synthesis provides new access to finding novel open-framework materials with interesting structures and physical properties.

One-dimensional metal phosphates often act as the building blocks for hybrid open-framework structures. Different metal phosphate chains, such as a corner-sharing 4-ring chain, an edge-sharing 4-ring ladder, and a zigzag chain composed of corner-sharing polyhedra, have been observed in phosphate-based hybrid structures.<sup>6</sup> For a specific hybrid structure, it always contains one type of inorganic chain as its building block. If different inorganic chains can be combined in the same

crystalline framework, more complicated open-framework structures are expected to be achieved. However, the growth of a hybrid framework with two or more building blocks is of great challenge because such a hybrid structure is generally more difficult for molecular recognition and a self-repairing process during crystallization.<sup>7</sup> Here we report the solvent-free synthesis of a new open-framework hybrid solid, namely,  $\text{H}_2\text{pip}\cdot\text{Mn}_5(\text{HPO}_4)_3(\text{C}_2\text{O}_4)_3(\text{H}_2\text{O})_2$  (**1**; pip = piperazine), which contains two different types of manganese phosphate chains as its building blocks. For a comparative study, its structural analogue, formulated as  $\text{H}_2\text{pip}\cdot\text{Mn}_4(\text{HPO}_4)_2(\text{C}_2\text{O}_4)_3(\text{H}_2\text{O})_2$  (**2**) and which only contains one type of inorganic chain, is also presented.

Blocklike crystals of compound **1** were obtained together with sticklike crystals of compound **2** by heating a mixture of piperazine,  $\text{Mn}(\text{H}_2\text{PO}_4)_2\cdot 2\text{H}_2\text{O}$ , and  $\text{H}_2\text{C}_2\text{O}_4\cdot 2\text{H}_2\text{O}$  in a molar ratio of 1:1.5:3 at 150 °C for 8 days. The two compounds were manually separated under an optical microscope (11% yield for **1** and 42% yield for **2** based on manganese). The yield of **1** could be improved to 46% by variation of the molar ratio of the starting materials. The phase purity of each as-synthesized compound is confirmed by powder X-ray diffraction (XRD) and CHN elemental analysis. Thermogravimetric analysis (TGA) shows that compound **1** remains stable up to 270 °C. Compound **2** loses its crystalline water molecules in the temperature region 185–235 °C (observed 4.1%; expected 4.5%). The framework starts to decompose at 270 °C.

Compound **1** crystallizes in the triclinic space group  $P\bar{1}$  (No. 2).<sup>8</sup> The asymmetric unit contains five manganese atoms, three  $\text{HPO}_4$  tetrahedra, three oxalate ligands, two water molecules, and one diprotonated pip cation. The linkages between manganese atoms,  $\text{HPO}_4$  tetrahedra, and oxalate ligands create a three-dimensional open-framework structure (Figure 1a). Viewed along the [100] direction, there are 8-ring channels delimited by four  $\text{MnO}_6$  octahedra, two  $\text{HPO}_4$  tetrahedra, and two oxalate ligands. The pore size of the 8-ring channel is about  $6.2 \times 7.0 \text{ \AA}^2$  (measured from the distances between two oxygen atoms across the window). The doubly protonated pip cations are well ordered within the channel, which occupy 19.6% of the unit cell volume. They form hydrogen bonds with framework oxygen atoms, with the shortest  $\text{N}\cdots\text{O}$  distances in the region of 2.754(4)–2.859(4) Å.

The most interesting structural feature of compound **1** is the presence of two types of manganese phosphate chains as its

Received: October 29, 2014

Published: December 16, 2014



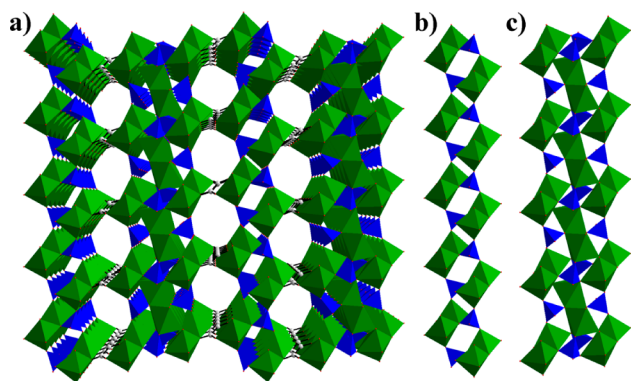


**Figure 1.** (a) Perspective view of the framework structure of **1** constructed from two types of manganese phosphate chains: (b) type I building block; (c) type II building block. Color code:  $\text{MnO}_6$  octahedra, green;  $\text{PO}_4$  tetrahedra, blue; oxygen, red; carbon, gray.

building blocks. As seen in Figure 1b, the connections of  $\text{Mn}(1)\text{O}_6$  octahedra,  $\text{Mn}(2)\text{O}_6$  octahedra, and  $\text{HP}(1)\text{O}_4$  tetrahedra result in the formation of a type I chainlike building block. Such an inorganic chain features isolated  $\text{Mn}_2\text{O}_{10}$  dimers linked by  $\text{HPO}_4$  tetrahedra. A type II inorganic chain is constructed from  $\text{Mn}(3)\text{O}_6$ ,  $\text{Mn}(4)\text{O}_6$ ,  $\text{Mn}(5)\text{O}_6$ ,  $\text{HP}(2)\text{O}_4$ , and  $\text{HP}(3)\text{O}_4$  polyhedra (Figure 1c). The inorganic chain features an infinite  $\text{Mn}-\text{O}-\text{Mn}$  chain constructed from corner-sharing  $\text{Mn}_2\text{O}_{10}$  dimers. The two kinds of chainlike building blocks are further cross-linked by oxalate ligands to form a three-dimensional structure.

If only the type I chain acts as the inorganic building block, the framework structure of **2** will be obtained. Single-crystal XRD analysis reveals that this compound is isostructural to several open-framework  $\text{M}-\text{HPO}_4-\text{C}_2\text{O}_4$  ( $\text{M} = \text{Mn},^9 \text{Fe},^{10}$  and  $\text{Co}^{11}$ ) compounds obtained under hydrothermal conditions. It has a three-dimensional framework with 8-ring channels along the  $[100]$  direction. The organic cations are accommodated within the channels, which occupy 22.1% of the unit cell volume. It is worth noting that the framework structure only consists of the type I inorganic chain as the building block.

To gain insight into the topological structures of **1** and **2**, it is instructive to view  $\text{Mn}_4\text{P}_2$  (Figure 2a) and  $\text{Mn}_6\text{P}_4$  (Figure 2b) clusters as the 6-connected nodes in (c) the pcu topology of **1**. Compound **2** has the same pcu topology with the  $\text{Mn}_4\text{P}_2$  clusters as the nodes.

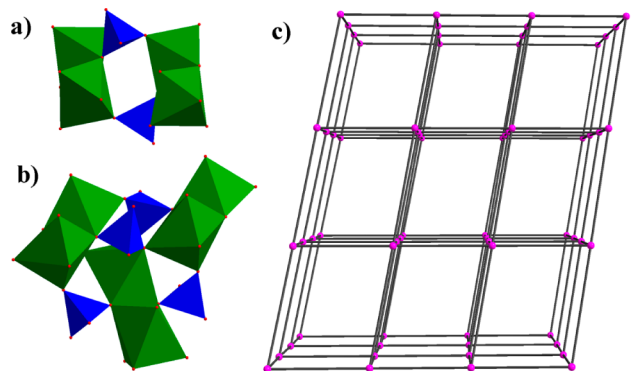


**Figure 2.** View of (a) the  $\text{Mn}_4\text{P}_2$  and (b)  $\text{Mn}_6\text{P}_4$  clusters as the 6-connected nodes in (c) the pcu topology of **1**. Compound **2** has the same pcu topology with the  $\text{Mn}_4\text{P}_2$  clusters as the nodes.

oxalate ligands, giving rise to a three-dimensional structure with a pcu topology (Figure 2c). In the case of **1**, the  $\text{Mn}_4\text{P}_2$  and  $\text{Mn}_6\text{P}_4$  clusters coexist in the structure with a ratio of 50:50. In the case of **2**, all of the 6-connected nodes are occupied by the  $\text{Mn}_4\text{P}_2$  clusters. Theoretically, the use of  $\text{Mn}_6\text{P}_4$  clusters as the nodes to construct an isorecticular structure formulated as  $\text{H}_2\text{pip} \cdot \text{Mn}_6(\text{HPO}_4)_4(\text{C}_2\text{O}_4)_3(\text{H}_2\text{O})_2$  is possible.

It has been demonstrated that the use of larger building blocks in a specific framework topology favors the formation of larger pore apertures.<sup>12</sup> For example, upon replacement of the T3 clusters in the UCR-7 network by the T4 clusters, the pore size will be enlarged from 18-ring to 24-ring.<sup>13</sup> Surprisingly, compound **1** displays the same pore aperture as that found in compound **2**, despite the fact that it possesses a larger inorganic building block than compound **2**. Careful analysis of the two structures reveals that every polyhedron in the  $\text{Mn}_4\text{P}_2$  cluster is involved in the pore structure, while the extra four polyhedra in the  $\text{Mn}_6\text{P}_4$  cluster do not appear in the 8-ring pore. The extra polyhedra play a role to thicken the inorganic walls of compound **1** but not to enlarge its pore size.

The temperature dependence of the magnetic susceptibility of the two compounds was measured in the temperature range 2–300 K (Figure 3). The magnetic moments ( $\mu_{\text{eff}}$ ) at 300 K per

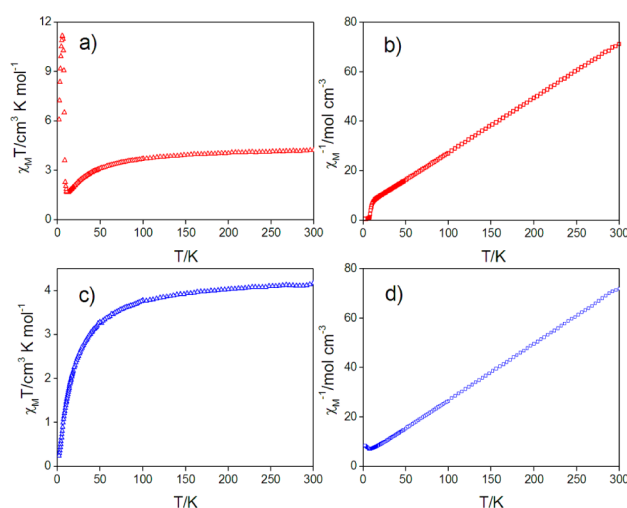


**Figure 3.** Temperature dependence of  $\chi_{\text{M}}T$  and  $\chi_{\text{M}}^{-1}$  for compounds **1** (a and b) and **2** (c and d).

mole of manganese atom are  $5.81 \mu_{\text{B}}$  for **1** and  $5.78 \mu_{\text{B}}$  for **2**, in agreement with the expected spin-only value of manganese(II) in the high-spin state ( $5.92 \mu_{\text{B}}$ ). For compound **1**, when the temperature is decreased, the  $\chi_{\text{M}}T$  values smoothly decrease to a minimum ( $1.66 \text{ cm}^3 \text{ K mol}^{-1}$ ) at 12 K. Below 12 K,  $\chi_{\text{M}}T$  sharply increases and reaches a maximum value ( $11.15 \text{ cm}^3 \text{ K mol}^{-1}$ ) at around 5.5 K before eventually falling to  $6.07 \text{ cm}^3 \text{ K mol}^{-1}$  at 2.0 K. This curve is similar as that of  $[\text{Mn}_3(\text{suc})_2(\text{ina})_2]_n$  which is characteristic of ferrimagnetic behavior caused by the structural factor of the  $\text{Mn}-\text{O}-\text{Mn}$  chain.<sup>14</sup> The thermal evolution of  $\chi_{\text{M}}$  follows the Curie–Weiss law at temperatures above 12 K, with  $C_{\text{m}} = 4.53 \text{ cm}^3 \text{ K mol}^{-1}$  and  $\theta = -23.1 \text{ K}$ . Similar to other isostructural manganese phosphate–oxalates,<sup>9</sup> compound **2** is an antiferromagnet. The  $\chi_{\text{M}}T$  value decreases continuously upon cooling and reaches a value of  $0.24 \text{ cm}^3 \text{ K mol}^{-1}$  at 2 K. The thermal evolution of  $\chi_{\text{M}}$  follows the Curie–Weiss law at temperatures above 8 K, with  $C_{\text{m}} = 4.46 \text{ cm}^3 \text{ K mol}^{-1}$  and  $\theta = -21.0 \text{ K}$ .

In summary, a new crystalline open-framework manganese phosphate–oxalate has been synthesized in a solvent-free flux of oxalic acid. The presence of two different types of manganese phosphate chains in the same hybrid framework is observed for the first time. It exhibits interesting ferrimagnetic behavior, which is quite different from the antiferromagnetic interactions between metal centers in its structural analogue that only contains one type of manganese phosphate chain. The present work demonstrates that a solvent-free approach may offer exciting opportunities to finding new hybrid open-framework materials with novel structures and appealing properties.

## ■ ASSOCIATED CONTENT

### ■ Supporting Information

X-ray data in CIF format, experimental details, additional figures, ORTEP plots, IR spectra, TGA curves, and powder XRD patterns. This material is available free of charge via the Internet at <http://pubs.acs.org>.

## ■ AUTHOR INFORMATION

### Corresponding Authors

\*E-mail: zhienlin@scu.edu.cn.

\*E-mail: huanghui@caep.ac.cn. Tel: +86 28 85412284. Fax: +86 28 85418451.

### Notes

The authors declare no competing financial interest.

## ■ ACKNOWLEDGMENTS

This work was supported by the NSFC (Grant 21171121) and the Program for New Century Excellent Talents in University (Grant NCET-12-0375).

## ■ REFERENCES

- (1) (a) Murugavel, R.; Choudhury, A.; Walawalkar, M. G.; Pothiraja, R.; Rao, C. N. R. *Chem. Rev.* **2008**, *108*, 3549–3655. (b) Wang, F.; Liu, Z.-S.; Yang, H.; Tan, Y.-X.; Zhang, J. *Angew. Chem., Int. Ed.* **2011**, *50*, 450–453.
- (2) (a) Natarajan, S.; Mandal, S. *Angew. Chem., Int. Ed.* **2008**, *47*, 4798–4828. (b) Morris, R. E.; Bu, X. *Nat. Chem.* **2010**, *2*, 353–361. (c) Zheng, S.-T.; Wu, T.; Chou, C.; Fuhr, A.; Feng, P.; Bu, X. *J. Am. Chem. Soc.* **2012**, *134*, 4517–4520.
- (3) (a) Choudhury, A.; Natarajan, S.; Rao, C. N. R. *Chem.—Eur. J.* **2000**, *6*, 1168–1175. (b) Lethbridge, Z. A. D.; Smith, M. J.; Tiwary, S. K.; Harrison, A.; Lightfoot, P. *Inorg. Chem.* **2004**, *43*, 11–13. (c) Yang, Y.-C.; Wang, S.-L. *J. Am. Chem. Soc.* **2008**, *130*, 1146–1147. (d) Wang, C.-M.; Wu, Y.-Y.; Hou, C.-H.; Chen, C.-C.; Lii, K.-H. *Inorg. Chem.* **2009**, *48*, 1519–1523. (e) Huang, S.-H.; Wang, S.-L. *Angew. Chem., Int. Ed.* **2011**, *50*, 5319–5322.
- (4) (a) Xiong, W.-W.; Athresh, E. U.; Ng, Y. T.; Ding, J.; Wu, T.; Zhang, Q. *J. Am. Chem. Soc.* **2013**, *135*, 1256–1259. (b) Zhang, G.; Li, P.; Ding, J.; Liu, Y.; Xiong, W.-W.; Nie, L.; Wu, T.; Zhao, Y.; Tok, A. I. Y.; Zhang, Q. *Inorg. Chem.* **2014**, *53*, 10248–10256. (c) Xiong, W.-W.; Zhang, G.; Zhang, Q. *Inorg. Chem. Front.* **2014**, *1*, 292–301.
- (5) (a) Pichon, A.; Lazuen-Garay, A.; James, S. L. *CrystEngComm* **2006**, *8*, 211–214. (b) Sakamoto, H.; Matsuda, R.; Kitagawa, S. *Dalton Trans.* **2012**, *41*, 3956–3961. (c) Wu, Q.; Wang, X.; Qi, G.; Guo, Q.; Pan, S.; Meng, X.; Xu, J.; Deng, F.; Fan, F.; Feng, Z.; Li, C.; Maurer, S.; Müller, U.; Xiao, F.-S. *J. Am. Soc. Soc.* **2014**, *136*, 4019–4025.
- (6) (a) Huang, S.-H.; Lin, C.-H.; Wu, W.-C.; Wang, S.-L. *Angew. Chem., Int. Ed.* **2009**, *48*, 6124–6127. (b) Chang, Y.-C.; Wang, S.-L. *J. Am. Chem. Soc.* **2012**, *134*, 9848–9851. (c) Nagarathinam, M.; Saravanan, K.; Phua, E. J. H.; Reddy, M. V.; Chowdari, B. V. R.; Vittal, J. J. *Angew. Chem., Int. Ed.* **2012**, *51*, 5866–5870.
- (7) (a) Christensen, K. E.; Shi, L.; Conradsson, T.; Ren, T.; Dadachov, M. S.; Zou, X. *J. Am. Chem. Soc.* **2006**, *128*, 14238–14239. (b) Wang, L.; Wu, T.; Bu, X.; Zhao, X.; Zuo, F.; Feng, P. *Inorg. Chem.* **2013**, *52*, 2259–2261.
- (8) Crystal data for **1**,  $C_{10}H_{19}Mn_5N_2O_{26}P_3$ ,  $M = 950.88$ , triclinic, space group  $P\bar{1}$  (No. 2),  $a = 7.7266(3)$  Å,  $b = 7.9643(4)$  Å,  $c = 21.2205(8)$  Å,  $\alpha = 90.298(4)^\circ$ ,  $\beta = 92.209(3)^\circ$ ,  $\gamma = 90.805(4)^\circ$ ,  $V = 1304.72(10)$  Å<sup>3</sup>,  $Z = 2$ ,  $D_c = 2.420$  g cm<sup>-3</sup>,  $\mu = 2.658$  mm<sup>-1</sup>, 10709 reflections measured, 5309 unique ( $R_{int} = 0.0291$ ). Final wR2 (all data) = 0.0756, final R1 = 0.0336. Crystal data for **2**,  $C_{10}H_{18}Mn_4N_2O_{22}P_2$ ,  $M = 799.96$ , triclinic, space group  $P\bar{1}$  (No. 2),  $a = 7.7895(3)$  Å,  $b = 8.0754(5)$  Å,  $c = 9.7286(6)$  Å,  $\alpha = 75.902(5)^\circ$ ,  $\beta = 79.142(4)^\circ$ ,  $\gamma = 86.695(4)^\circ$ ,  $V = 582.86(6)$  Å<sup>3</sup>,  $Z = 1$ ,  $D_c = 2.279$  g cm<sup>-3</sup>,  $\mu = 19.577$  mm<sup>-1</sup>, 6223 reflections measured, 2077 unique ( $R_{int} = 0.0504$ ). Final wR2 (all data) = 0.1375, final R1 = 0.0483.
- (9) (a) Lethbridge, Z. A. D.; Tiwary, S. K.; Harrison, A.; Lightfoot, P. *J. Chem. Soc., Dalton Trans.* **2001**, 1904–1910. (b) Yu, R.; Xing, X.; Saito, T.; Azuma, M.; Takano, M.; Wang, D.; Chen, Y.; Kumada, N.; Kinomura, N. *Solid State Sci.* **2005**, *7*, 221–226.
- (10) (a) Choudhury, A.; Natarajan, S.; Rao, C. N. R. *J. Solid State Chem.* **1999**, *146*, 538–545. (b) Chang, W.-J.; Lin, H.-M.; Lii, K.-H. *J. Solid State Chem.* **2001**, *157*, 233–239. (c) Meng, H.; Li, G.-H.; Xing, Y.; Yang, Y.-L.; Cui, Y.-J.; Liu, L.; Ding, H.; Pan, W.-Q. *Polyhedron* **2004**, *23*, 2357–2362.
- (11) Choudhury, A.; Natarajan, S. *Solid State Sci.* **2000**, *2*, 365–372.
- (12) (a) O'Keeffe, M.; Eddaoudi, M.; Li, H.; Reineke, T.; Yaghi, O. M. *J. Solid State Chem.* **2000**, *152*, 3–20. (b) Férey, G. *J. Solid State Chem.* **2000**, *152*, 37–48.
- (13) (a) Wang, C.; Bu, X.; Zheng, N.; Feng, P. *Chem. Commun.* **2002**, 1344–1345. (b) Zheng, N.; Bu, X.; Feng, P. *J. Am. Chem. Soc.* **2003**, *125*, 1138–1139.
- (14) Zeng, M.-H.; Wu, M.-C.; Liang, H.; Zhou, Y.-L.; Chen, X.-M.; Ng, S.-W. *Inorg. Chem.* **2007**, *46*, 7241–7243.